

Controllable Doping Characteristics for WS_xSe_y Monolayers Based on the Tunable S/Se Ratio

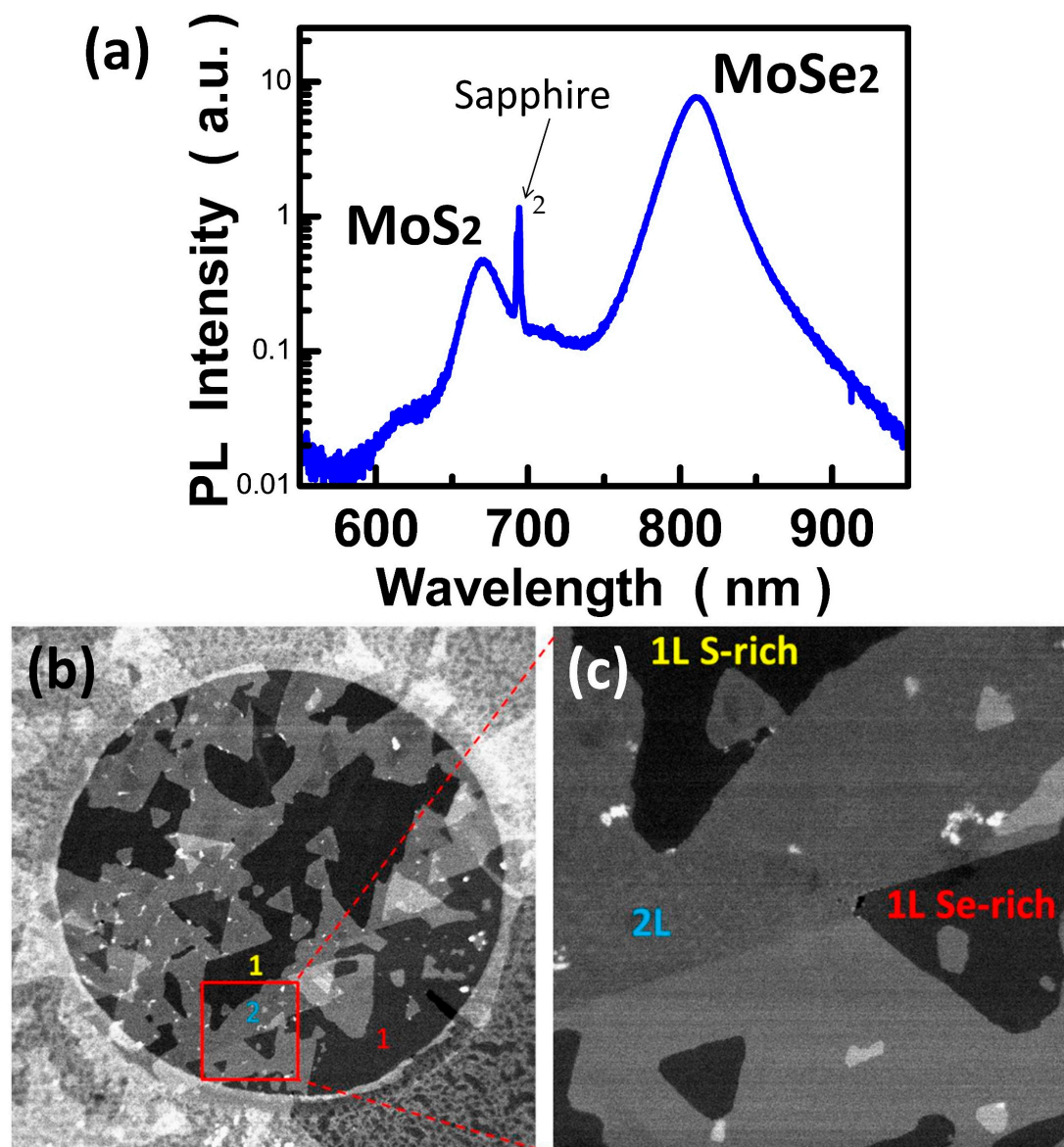


Figure S1. (a) PL spectrum showing the two characteristic peaks belonging to MoS₂ and MoSe₂ respectively. (b,c) The bright-field TEM images showing the distinguishable S- and Se-rich parts in the WS_xSe_y .

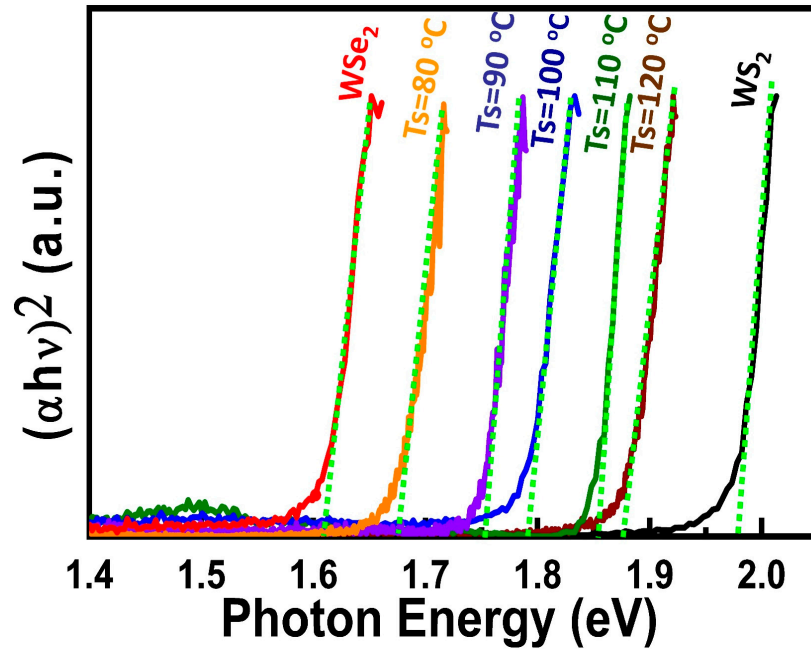


Figure S2. Plots of the $(\alpha h\nu)^2$ versus photon energy ($h\nu$) for direct inter-band transitions of WS_2 , WS_xSe_y , and WSe_2 monolayers whose intercepts of tangents represent the band gap energy.

The optical E_g based on direct inter band transitions can be derived from the absorption coefficient equation as followed: $\alpha = B_d(h\nu - E_g)^{1/2}/h\nu$, where α is the optical absorption coefficient, B_d is the absorption constant, h is the Planck constant and ν is the frequency of the incident photon. Figures S2 show plots of $(\alpha h\nu)^2$ versus the photon energy ($h\nu$) for the WS_2 , WS_xSe_y at $T_s=120, 110, 100, 90$ to 80 °C, and WSe_2 , where the linear fit intercepts representing the optical E_g are 1.97, 1.88, 1.85, 1.79, 1.75, 1.67, and 1.61 eV, respectively.

Table S1. The chemical stoichiometries for the WS_2 , WS_xSe_y at $T_s=120, 110, 100, 90$ to 80 °C, and WSe_2 monolayers.

		WS_2	$T_s=120^\circ C$	$T_s=110^\circ C$	$T_s=100^\circ C$	$T_s=90^\circ C$	$T_s=80^\circ C$	WSe_2
ratio	W	1	1	1	1	1	1	1
	S	2.20	1.87	1.66	1.54	1.12	0.88	0
	Se	0	0.31	0.40	0.48	1.00	1.39	1.77

Table S2. The band gap (E_g), work function (ϕ), and E_F-E_v for the WS_2 , WS_xSe_y at $T_s=120, 110, 100, 90$ to 80 °C, and WSe_2 monolayers.

		WS_2	$T_s=120^\circ C$	$T_s=110^\circ C$	$T_s=100^\circ C$	$T_s=90^\circ C$	$T_s=80^\circ C$	WSe_2
Bandgap energy (eV)		1.97	1.88	1.85	1.79	1.75	1.67	1.61
Work function (eV)		4.31	4.17	4.06	4.03	4	3.96	3.95
E_F-E_v (eV)		0.735	0.835	0.885	0.90	0.91	0.91	0.96